VIBRATION RESPONSE CHARACTERISTICS OF ROCKING PILLAR BASE ISOLATION SYSTEM SUITABLE FOR MASONRY HOUSES

Naoki Funaki[1], Tomomi Fujita[2], Norio Hori[3], Norio Inoue[4] and Shigeya Kawamata[5]

[1] *Lecturer, Dept. of Architecture, Tohoku Institute of Technology, Sendai, JAPAN*
[2] *Visiting Researcher, Dept. of Architecture, Tohoku Institute of Technology, Sendai, JAPAN*
[3] *Assistant Professor, School of Engineering, Tohoku University, Sendai, JAPAN*
[4] *Professor, School of Engineering, Tohoku University, Sendai, JAPAN*
[5] *Professor Emeritus, Dept. of Architecture, Tohoku Institute of Technology, Sendai, JAPAN*
Email: funaki@tohtech.ac.jp, fujita@tohtech.ac.jp

ABSTRACT :

In developing countries of seismic area, many people have to live in traditional masonry houses of stones, bricks and concrete blocks. Though collapse of the houses is one of the most tragic losses of human lives, shift of the houses to construction based on modern engineering is difficult by socioeconomic reason. The authors have been developing a new base isolation system suitable for masonry houses utilized rocking pillar foundation. This paper describes structural scheme of the base isolation system and presents results of vibration test of a reduced scale test specimen. Based on the obtained test results, the basic characteristics of vibration response and seismic performance of the newly developed system are discussed. Also, numerical simulation by a developed program is carried out. To verify the validity of the program, the results of shaking table test are compared with those of the corresponding numerical simulation by the program.

KEYWORDS: Base Isolation, Rocking Pillar, Lead Damper, Masonry House
Shaking Table Test, Numerical Analysis

1. INTRODUCTION

In developed countries of seismic area, dwelling houses and apartment houses are built based on modern construction technique and maintain some level of seismic resistance. Recent application of seismic control technique to these houses will conspicuously advance the level of safety and reliability against earthquake. In contract, many people in developing countries have to live, by technical and economical reasons, in traditional masonry houses. The earthquake of M6.5, which took place in Iran on December 26, 2003, totally destroyed the historical city of Bam killing 40,000 people. More recently, many casualties due to collapsing masonry houses in developing countries during earthquakes are reported. The disasters remind us it is one of the most urgent subjects of earthquake engineering to improve seismic resistance of the masonry houses in developing countries. However, it is not easy to shift the construction of these houses to the one of modern technology but dependence on local products of masonry material will not be changed. A possible solution of avoiding collapse of masonry houses is to implement base isolation devices to reduce input seismic force within the shearing strength of the masonry walls. To popularize the base isolation system widely in developing countries, the system must be so simple to manufacture in low cost and be installed in the site by non-skilled local laborers. Taking the above requirements into account, the authors have developed a new form base isolation system for masonry houses utilizing rocking pillar foundation [1]. The purpose of this paper is to verify the fundamental property of vibration response and investigate seismic performance of the system based on results of vibration test using reduced scale test specimen. Also, in the present paper the authors intend to expand the analytical method discussed earlier and to

state vibration response properties of the base isolation system in detail.

2. OUTLINE AND VIBRATIONAL PROPERTY OF THE BASE ISOLATION SYSTEM

Figure 1 shows a masonry house provided with the proposed base isolation system. The base isolation foundation consists of rocking pillars, dampers and caissons as illustrated in the Figure 2. Figure 3 shows geometry of the rocking pillar. By making radius of curvature of both end of the pillar, R, larger than half-length of the pillar, L, restoring moment occurs against rocking motion rotating around the bottom end of the pillar. Consequently, superstructure supported by the rocking pillars is subjected to slow lateral vibration of long period. Natural period of the system is derived from equilibrium of moment of inertia acting on the pillar and restoring moment of the pillar, as follows:

$$T = 2\pi\sqrt{\frac{2L^2}{(R-L)g}} \tag{2.1}$$

As shown in equation (2.1), natural period of the base isolation foundation does not depend on mass of the superstructure but is determined by dimension of the pillar, R and L. This property is attributed to restoring moment of the pillar is proportional to its vertical load. Accordingly, the present rocking pillar base isolation system is free from torsional vibration in principle because of the center of distributed restoring moment automatically coincides with the center of gravity of the superstructure.

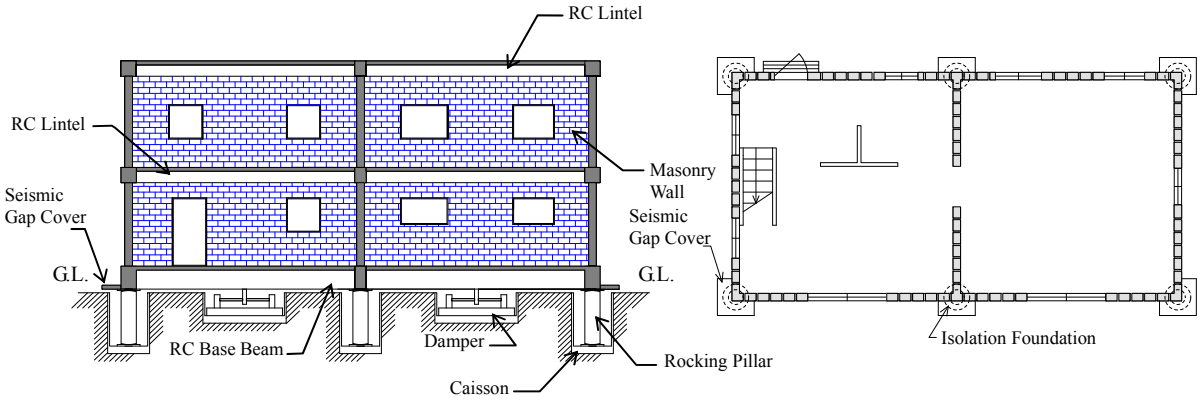

Figure 1 Plan and section of masonry house with isolation foundation

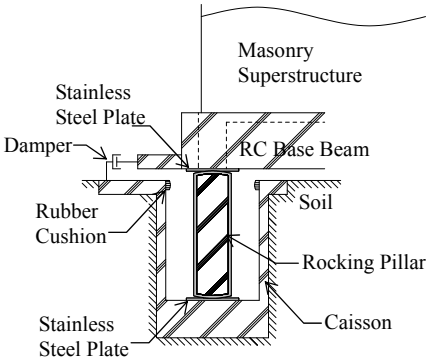

Figure 2 Scheme of isolation foundation

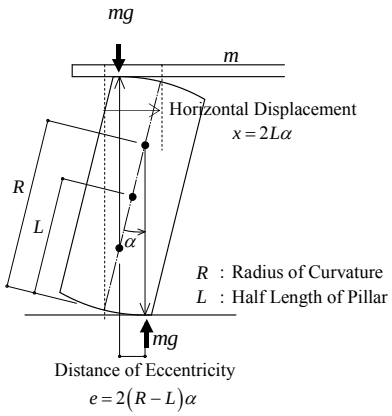

Figure 3 Geometry of rocking pillar

3. VIBRATION RESPONSE CHARACTERISTICS OF ISOLATION FOUNDATION SPECIMEN

3.1. Test Apparatus Description and Test Setup

Free vibration and shaking table tests were carried out on reduced scale test specimen of the isolation foundation system. Figure 4 shows detail of the test specimen and view of the apparatus on a shaking table. The superstructure was composed of a raft of steel beams and weight of steel plates mounted on it and was supported by four rocking pillars. Total mass of the weight was 1.4ton. To form the weight, steel plates were piled on the basement beams in X1 and X2 axes. The weights were arranged in two different types of pilling: symmetric and eccentric. In the former case, two piles having same mass of 0.55ton were placed, and in the latter case, two piles of different mass were located. Test case is listed in Table 3.1. The rocking pillar was formed by steel rod equipped with spherical bearings of R=20cm at the both ends. The length of the rocking pillar, 2L, was 34cm. The pillar was set on smooth stainless plate of 6mm thickness. The same plate was installed between the top of the pillar and the basement beam. Caisson was fabricated from transparent acrylic tube so that the rocking pillar was visible from outside. As shown in Figure 5, lead dampers were installed between the basement beams and the shaking table. The damper was made from flat lead plate shaped into a circular arc (Figure 6). To verify the resisting force characteristics of the damper, harmonic excitation tests were carried out both in strong axis and weak axis. Based on obtained test results, they took the forms of steady spindle shape and it was confirmed that the damper operated regularly for large amplitude and had high energy dissipation capacity.

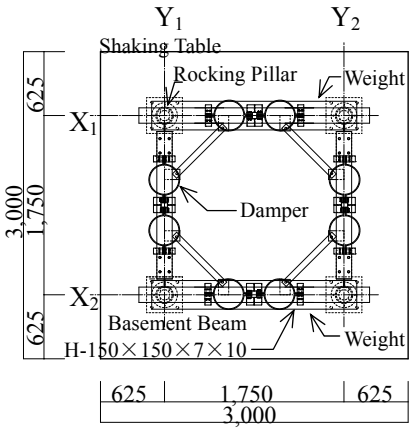

(a) Plan

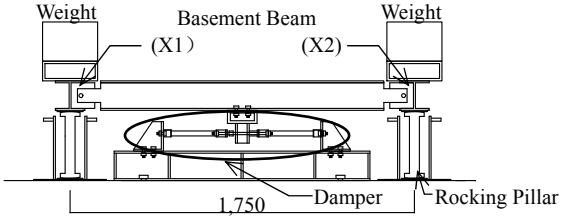

(b) Section

(c) View of test specimen on shaking table (Case 3)

Figure 4 Isolation foundation specimen (unit: mm)

Figure 5 Lead damper installed in test specimen

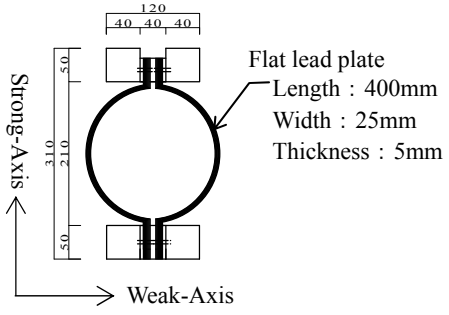

Figure 6 Detail of lead damper (unit: mm)

Table 3.1 Test cases

Test case	Number of installed steel plate		Mass eccentricity ratio*
	X_1 Beam	X_2 Beam	$X_1 : X_2$
Case1 (Symmetric type)	5	5	1 : 1.00
Case2 (Eccentric type)	4	6	1 : 1.36
Case3 (Eccentric type)	3	7	1 : 1.89
Case4 (Eccentric type)	2	8	1 : 2.71
Case5 (Eccentric type)	1	9	1 : 4.20

* Mass eccentricity ratio indicated in this Table include weight of basement beam

The instrumentation set-up that was used to measure the response of the test specimen to vibration tests is shown in Figure 7. Four accelerometers were fixed on the top of the basement beams (X_1, X_2, Y_1, Y_2) in order to measure response acceleration and a bidirectional accelerometer was attached at center of the shaking table to record input acceleration. Displacement of the basement beams relative to the shaking table was measured using laser displacement sensors and resisting force of the lead damper was measured by a load cell as shown in Figure 7(a).

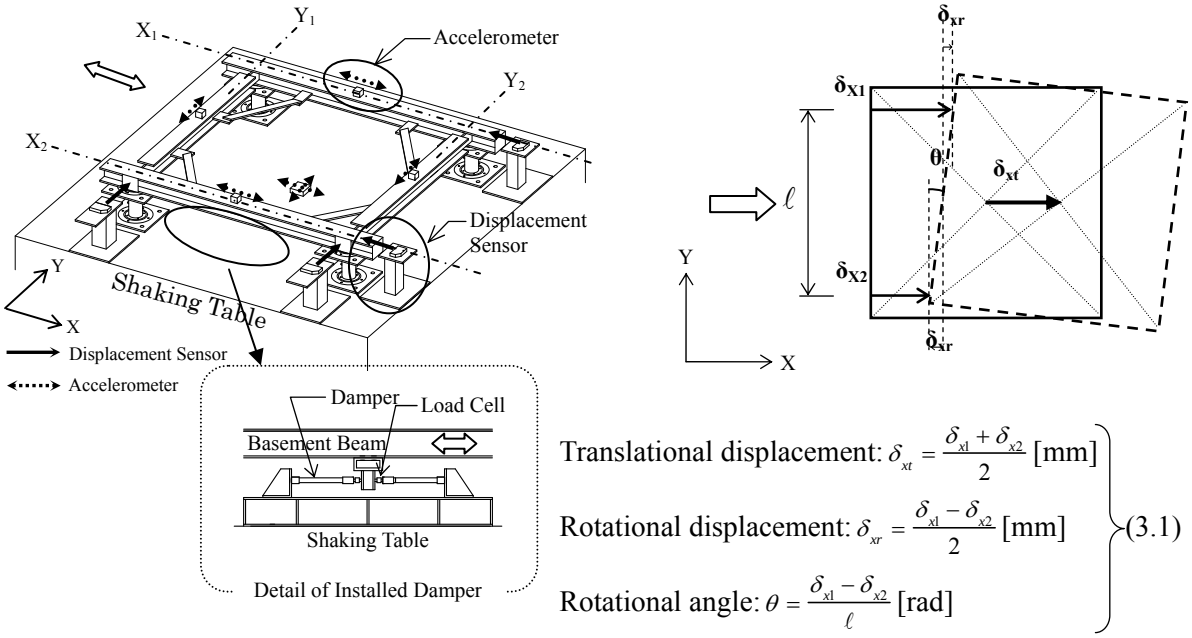

Translational displacement: $\delta_{xt} = \dfrac{\delta_{x1} + \delta_{x2}}{2}$ [mm]

Rotational displacement: $\delta_{xr} = \dfrac{\delta_{x1} - \delta_{x2}}{2}$ [mm]

Rotational angle: $\theta = \dfrac{\delta_{x1} - \delta_{x2}}{\ell}$ [rad] (3.1)

(a) Test setup (b) Translational and rotational displacement

Figure 7 Instrumentation set-up

As shown in Figure 7 (b), translational and rotational displacement of the basement beams in X axis, δ_{xt} and δ_{xr}, are calculated by Equation (3.1), where δ_{x1} and δ_{x2} indicate relative displacement of the basement beams in X_1 and X_2 axes respectively.

3.2. Free Vibration Test of Undamped Specimen

The test specimen without damper was subjected to free vibration tests in X direction through excitation by man power. Figures 8 and 9 show typical time histories of relative displacement along the X_1 and X_2 axes and rotational displacement of the basement beams for symmetric and eccentric cases. Table 3.2 lists estimated natural period and damping ratio based on the obtained test results. In spite of difference in arrangement of the weight, the basement beams along the X_1 and X_2 axes showed approximately similar time histories of relative displacement. Also, the maximum ratio of rotational displacement to relative displacement was less than 5%. Consequently, it was proved that the base isolation system is free from torsional vibration. Also, natural periods derived by test results agree approximately with calculated result by Equation (2.1). The system exhibited viscous type of damping and damping ratio took small value about 1% of critical damping.

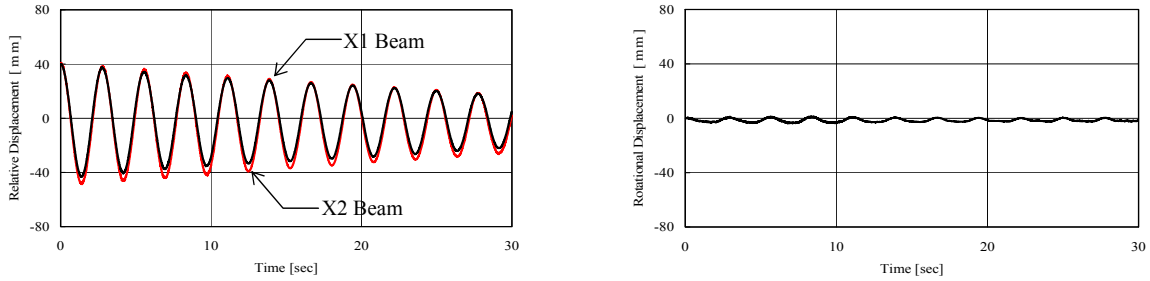

(a) Relative Displacement (b) Rotational Displacement

Figure 8 Free Vibration time histories, Symmetric weight

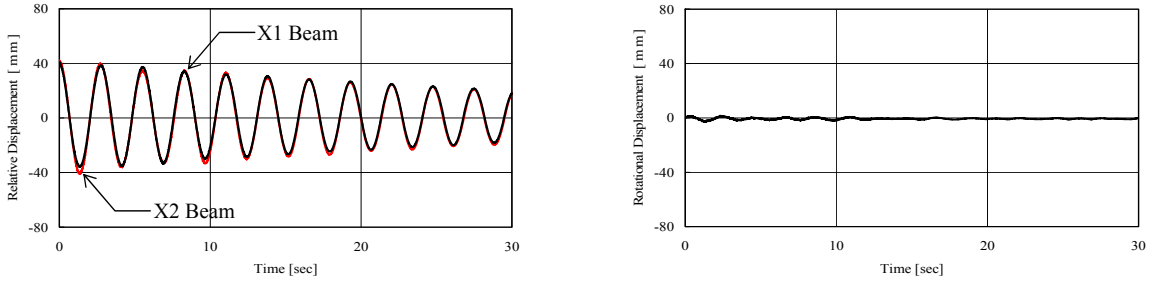

(a) Relative Displacement (b) Rotational Displacement

Figure 9 Free Vibration time histories, Eccentric weight (Case 3)

Table 3.2 Natural period and damping ratio

Test Case	Mass eccentricity ratio $X_1 : X_2$	Natural Period [sec]		Damping Ratio [%]
		Test	Theory	
Case 1 (Symmetric)	1 : 100	2.78	2.78	1.20
Case 3 (Eccentric)	1 : 1.36	2.77		1.07
Case 5 (Eccentric)	1 : 4.20	2.71		1.15

3.3. Shaking Table Test of Damped Specimen

To investigate the basic characteristics of earthquake response and effect mass eccentricity of superstructure have on seismic performance of the system, recorded earthquake waves were input to the shaking table. El centro NS component of the 1940 Imperial Valley Earthquake was used as input motion. The excitation was one-directional along X axis. Time axis of the input earthquake waves were compressed into 1/2 of the original considering that the test specimen was reduced scale model. As representative test results obtained by excitation of maximum inputs, time histories for eccentric test case (Case 3) are presented in Figure 10. The data of peak response to maximum input are listed in Table 3.3. In all cases, the response acceleration was largely decreased from the one of shaking table, the range of amplification factors being from 0.07 to 0.11 to maximum input. Accordingly, it can be considered that the developed isolation system demonstrates superior seismic performance. The difference in behavior of the test specimen for each case investigates based on the test results. In the case of symmetric weight, the specimen exhibited steady state vibration without rotational effect, while in the case of eccentric weight, the rotational displacement of the basement beam was two to three times larger than the symmetric case. As indicated in previous section, the restoring moment of the pillar is proportional to its vertical load. Therefore, the center of distributed restoring moment automatically coincides with the center of gravity of the superstructure. Consequently, eccentric mass of the superstructure does not contribute to the increase in gyration of the base isolation foundation. In the specimen with dampers, to prevent occurrence of torsional vibration, the center of rigidity of the damper in plane is also required to coincide with the center of gravity of the superstructure. Since the dampers were set up symmetrically to the test specimen in this experiment, the growth of torsional vibration was unavoidable. Figure 11 shows relation between response ratio and maximum translational displacement under each input level. The response ratio is defined as ratio of maximum

response of the eccentric test specimen to maximum response of the symmetric one under same input level. As Figure 11 shows, maximum response displacement of all eccentric test specimens approximately equal that of symmetric case with increasing input level. Maximum response acceleration of X_2 beam which was piled heavier weight show nearly equal to that of symmetric cases. On the other hand, response acceleration of the X1 beam increases as the mass of the weight decreases. However, even in such cases, response acceleration amplification factor becomes small as 0.15.

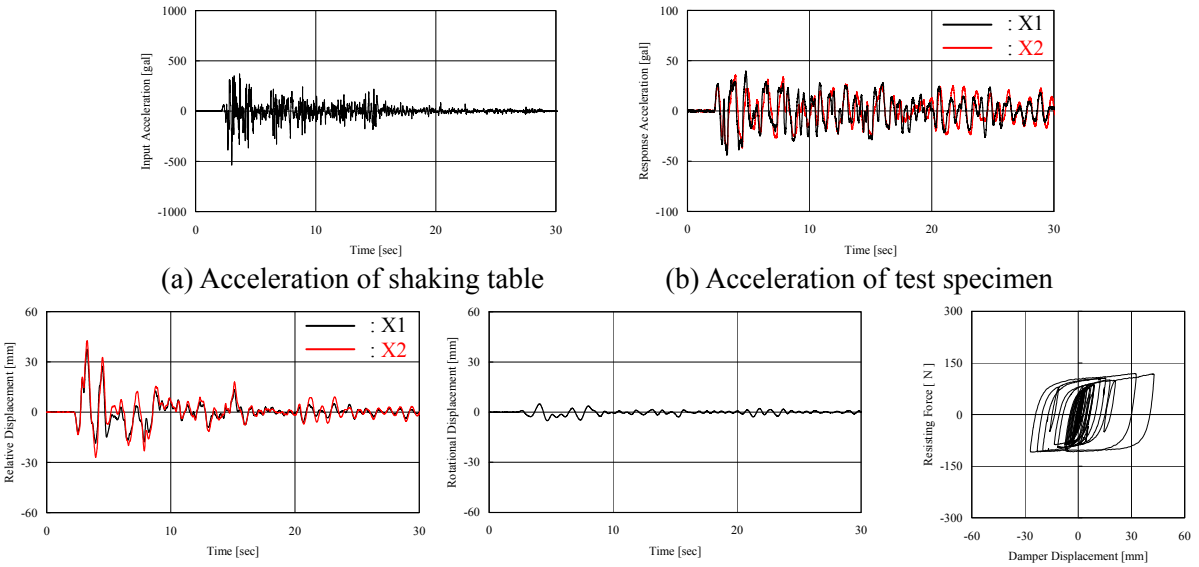

(a) Acceleration of shaking table (b) Acceleration of test specimen

(c) Relative displacement of test specimen (d) Rotational displacement of test specimen (e) Displacement orbit of test specimen

Figure 10 Response to excitation of earthquake inputs (Case 3)

Table 3.4 Response to maximum earthquake input

Test Case	Acceleration of Shaking Table [gal]	Maximum Response Acceleration [gal]		Amplification Factor of Acceleration		Maximum Relative Displacement [mm]			Rotational Displacement δ_{xr} [mm]	Maximum Torsional Angle θ [$\times 10^{-3}$rad]
		X1	X2	X1	X2	X1	X2	Translation Displacement		
Case 1	490.0	40.75	40.96	0.08	0.08	37.80	39.86	38.83	1.49	1.70
Case 2	498.6	39.69	40.86	0.08	0.08	35.74	39.46	37.60	3.39	3.87
Case 3	533.9	43.99	41.74	0.08	0.08	37.58	42.76	40.17	5.08	5.81
Case 4	496.0	49.98	40.08	0.10	0.08	33.58	40.80	37.20	6.89	7.87
Case 5	549.2	58.02	40.57	0.11	0.07	34.64	43.44	39.04	9.01	10.30

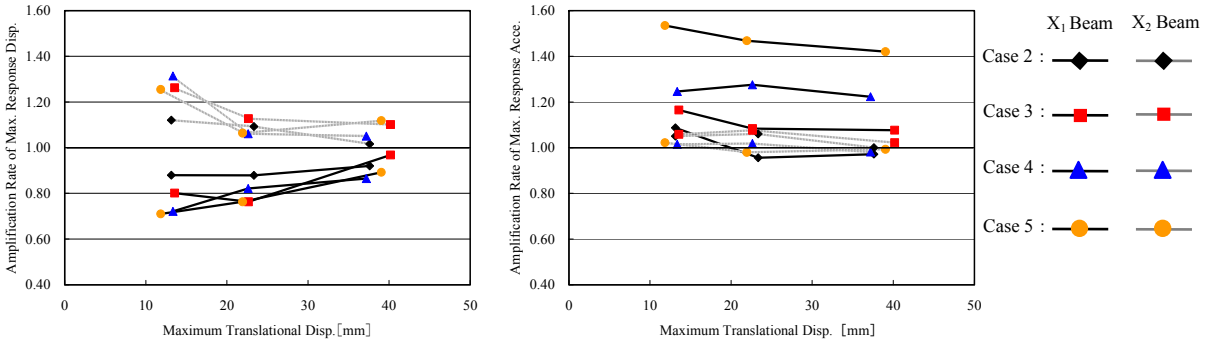

(a) Response Displacement (b) Response Acceleration

Figure 11 Response ratios for eccentric test cases

4. VIBRATION RESPONSE ANALYSIS

4.1. Vibration System and Equation of Motion

To investigate earthquake response characteristics of the base isolation system, a time integration program was developed based on Newmark β method. To verify the validity of the analytical method, the results of shaking table test were compared with those of corresponding numerical simulation by the analysis program. The base isolation system has three degrees of freedom, two of which are translations and one rotation about a vertical axis, it can be modeled by vibration system as shown in Figure 12. As for the present lead damper system, the hysteretic resisting force can be idealized by a bilinear model with yield-judgment straight line shown in Figure 13, where parameters are obtained from harmonic excitation test results of the damper.

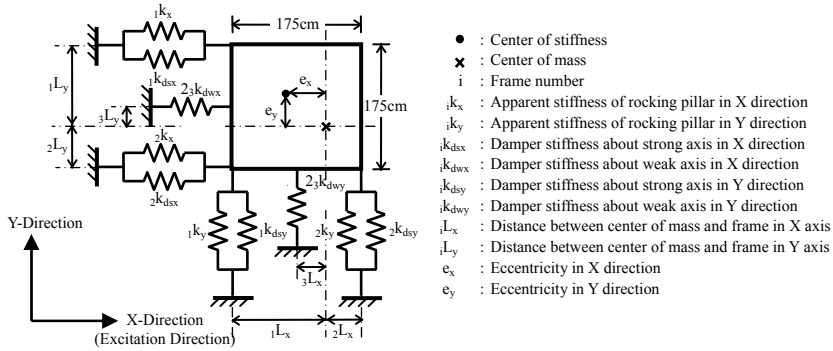

Figure 12 Vibration system of the test specimen

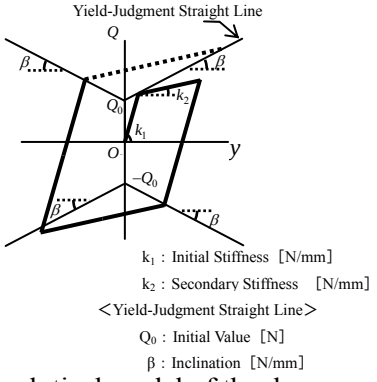

Figure 13 Analytical model of the damper

Apparent horizontal stiffness of the rocking pillar, $_ik_x$ and $_ik_y$, illustrated in Figure 12, are taken to be

$$K_i = m_i\left(\frac{2\pi}{T}\right)^2 \tag{4.1}$$

where m_i is mass carried on the each rocking pillar and T is natural period of the pillar derived by Equation (2.1). To apply time integration analysis to the model in Figure 12, equation of motion for the vibration system is written as follows for n-th step of discrete time increment.

$$\begin{bmatrix} m & 0 & 0 \\ 0 & m & 0 \\ 0 & 0 & I \end{bmatrix}\begin{Bmatrix} \ddot{x}_{(n)} \\ \ddot{y}_{(n)} \\ \ddot{\theta}_{(n)} \end{Bmatrix} + \begin{bmatrix} K_x & 0 & K_x\cdot e_y \\ 0 & K_y & K_y\cdot e_x \\ K_x\cdot e_y & K_y\cdot e_x & K_\theta \end{bmatrix}\begin{Bmatrix} x_{(n)} \\ y_{(n)} \\ \theta_{(n)} \end{Bmatrix} = -\begin{bmatrix} m & 0 & 0 \\ 0 & m & 0 \\ 0 & 0 & I \end{bmatrix}\begin{Bmatrix} \ddot{x}_{0(n)} \\ \ddot{y}_{0(n)} \\ \ddot{\theta}_{0(n)} \end{Bmatrix} \tag{4.2}$$

where m is a total mass of superstructure, I is a rotation inertia, K_x and K_y are horizontal stiffness of the base isolation foundation in X and Y direction and K_θ is a torsional stiffness.

Table 4.1 Fundamental parameters of the test specimen used in numerical simulation

		Strong Axis : k_{ds}	Weak Axis : k_{dw}
Damper	Initial stiffness : k_1 [N/mm]	38.2	6.69
	Secondary stiffness : k_2 [N/mm]	0.49	0.17
	Initial value : Q_0 [N]	78.4	29.4
	Inclination : β [N/mm]	1.47	0.29
Vibration System	Total Mass : m [ton]	1.30	
	Natural period of the pillar : T [sec]	2.783	
	Overall stiffness of the pillar : Σ_iK_x, Σ_iK_y [N/mm]	6.63	
	Damping ratio : h [%]	0	
	Rotation inertia : I [$\times 10^5$ N・mm^2]	Case 1 : 147.29 Case 2 : 133.63 Case 3 : 136.44 Case 4 : 112.13 Case 5 : 98.95	
Time step : Δt [sec]		0.005	

The parameters of the test specimen including the damper were determined according to the test data as listed in Table 4.1. Damping effect of the rocking pillar was ignored in this analysis since the test specimen without damper exhibited low damping. For input ground motion, measured shaking table acceleration was used.

4.2. Results of Analysis

Figure 14 shows typical examples of the shaking table test results together with the results of the corresponding numerical simulation. It can be seen that analytical results simulated the test results comparatively well.

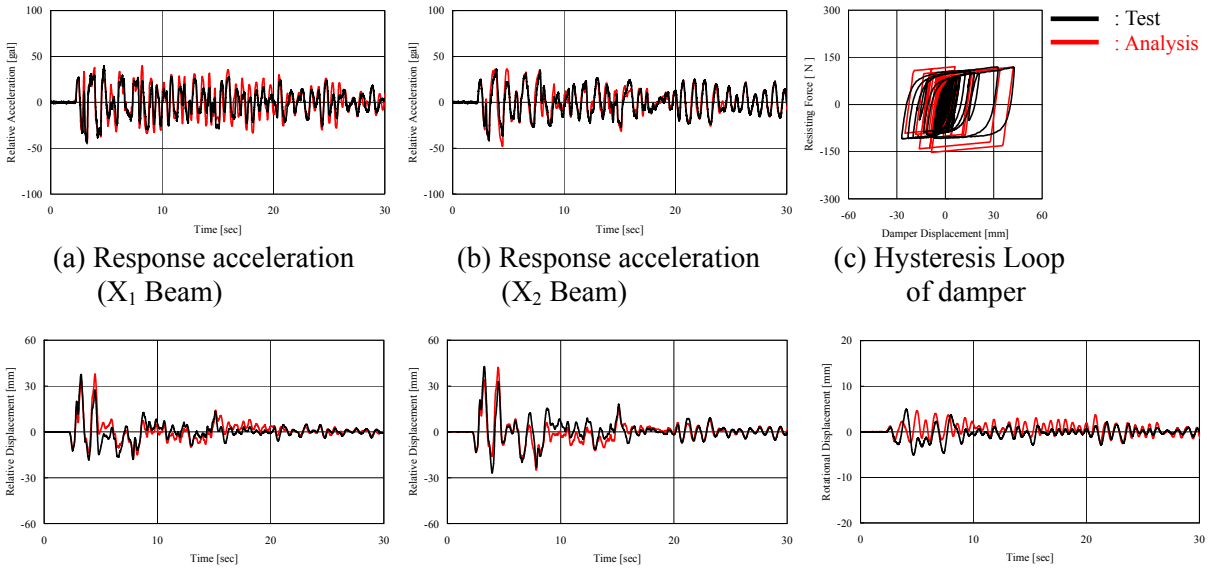

(a) Response acceleration (X_1 Beam) (b) Response acceleration (X_2 Beam) (c) Hysteresis Loop of damper

(d) Response displacement (X_1 Beam) (e) Response displacement (X_2 Beam) (f) Rotational displacement

Figure 14 Comparison of response to El Centro NS wave, Eccentric weight (Case 3)

5. CONCLUSION

Vibration tests were conducted with regard to a 1/4 scale model of a base isolation system supported by rocking pillars which was formerly proposed by the authors as a new form of base isolation suitable to masonry houses in developing countries [1]. The results of free vibration indicated that the natural period of fundamental mode coincided with the theoretical period which is determined by the geometry of the rocking pillar independently from supported mass of the superstructure. Shaking table tests by earthquake wave input attained very low acceleration amplification factors, limiting being from 0.07 to 0.11. Also, the eccentric mass of superstructure exerted only a minimal influence on vibration response of the base isolation system. Numerical response analysis by the use of developed program showed fairly good coincidence with the results of the earthquake wave excitation tests. Summarizing the above, proposed base isolation system seems to offer a promising device to limit the earthquake response of masonry houses within the shearing strength of the masonry walls.

REFERENCES

[1] Shigeya KAWAMATA, Naoki FUNAKI, Norio HORI, Tomomi FUJITA and Norio INOUE. (2004), Base Isolation System Suitable for Masonry Houses, Proceedings of the 13th World Conference on Earthquake Engineering, Paper 668, Vancouver, B.C., Canada